

GEOL. CROAT.	50/1	17 - 25	7 Figs.	2 Tabs.		ZAGREB 1997
--------------	------	---------	---------	---------	--	-------------

Glaucanitic Materials from Lower Miocene Macelj-Sandstones of the Hrvatsko Zagorje, North-Western Croatia

Neven TADEJ, Dragutin SLOVENEK, Josip TIŠLJAR and Ivica INKRET

Key words: Macelj-sandstones, Glaucanitic materials, Glaucanite, XRD powder patterns, Chemical composition, Thermal analysis, Hrvatsko Zagorje, Croatia.

Abstract

The Lower Miocene Macelj-sandstones, from the western part of Hrvatsko Zagorje, are green in colour with variable amounts of glaucanitic grains. This paper presents the results of mineralogical and some petrological analysis of three characteristic samples of these sandstones.

The natural sandstone samples were analysed by polarising microscope and by X-ray powder diffraction (XRD). After separation, the pure or almost pure glaucanitic materials were analysed by XRD, chemical analysis and thermal analysis (TG, DTA and DTG). The results show variation, not only in the glaucanitic material of the sandstone samples, but also within individual samples. The amount of smectite layers varies from <5% to approximately 40% depending on the degree of order and the stage of glaucanite evolution. This is indicated by the contents of K, Al, Fe, adsorbed water and cation exchange capacity as well as XRD powder patterns.

1. INTRODUCTION

The Macelj-sandstones are located in the western part of the Hrvatsko Zagorje region in north-western Croatia, and in adjacent eastern Slovenia. The name Macelj-sandstones has been used ever since they were described by GORJANOVIĆ-KRAMBERGER (1904) in the explanatory text for the geological map, sheet Rogatec-Kozje, as "greenish-grey tuffaceous sandstones indicating a shallow-marine environment". These sandstones outcrop in the Hrvatsko Zagorje region between Mt. Strahinšćica and Mt. Ivanščica in the south, and Mt. Ravna Gora in the north, covering a total surface area of about 130 km² (Fig. 1). This formation is predominantly composed of shallow-marine clastics, several hundred metres thick, characterised by glaucanite-bearing sandstones with subordinate quantities of conglomerate, tuffitic sandstone, tuff, and clay (TIŠLJAR & ŠIMUNIĆ, 1978; ŠIMUNIĆ et al., 1990). The stratigraphic position of these sedimentary rocks is

Lower Miocene (from Egerian to Karpathian), during which sedimentation creating barrier sand bars predominated, occasionally interrupted by dacite-andesite explosive volcanism. The volcanism began to cease by the end of this period, and a new transgression and tectonic movements prevented deposition of clastic sediments, and increased carbonate sedimentation (ŠIMUNIĆ et al., 1990).

The Macelj-sandstones are of homogenous mineral composition with variation expressed through grain size and relative percentages of volcanoclastic material, matrix and cement. The detrital composition indicates source areas composed mostly of sedimentary rocks and schists. In the tuffitic sandstones the distinction between resedimented and directly deposited volcanoclastic material is ambiguous due to intensive chloritization and glaucanitization. The matrix composition and texture seem to indicate direct deposition of volcanic ash, which was produced by periodic eruptions in the adjacent areas (TIŠLJAR & ŠIMUNIĆ, 1978).

This paper represents introductory work in the investigation of glaucanitic materials of the Macelj-sandstones and the analysis of these materials from three typical sandstone samples. Sample M3 was taken from the outcrop (lower part of the Lower Miocene massive Macelj-sandstones) on the Đurmanec-Macelj road, near the border between Croatia and Slovenia (the border crossing Macelj). Sample RG was obtained from a drill core (at 31.5 m depth) from an exploratory well situated south-west of the village of Strupari, south of Mt. Ravna Gora. Sample MT was taken from an outcrop (upper part of the Lower Miocene cross-bedded Macelj-sandstones) on the road near Donji Macelj. The sample locations are presented on Fig. 1.

Analogous to ŠRODOŃ's (1984) definition for illitic materials, in this paper we used the term glaucanitic material to refer to both glaucanite and to interstratified glaucanite-smectite, as well as to their mixture.

2. DESCRIPTION AND MINERAL COMPOSITIONS OF SANDSTONE SAMPLES

The samples of the Macelj-sandstones were analysed by polarizing microscope and X-ray powder diffraction (XRD).

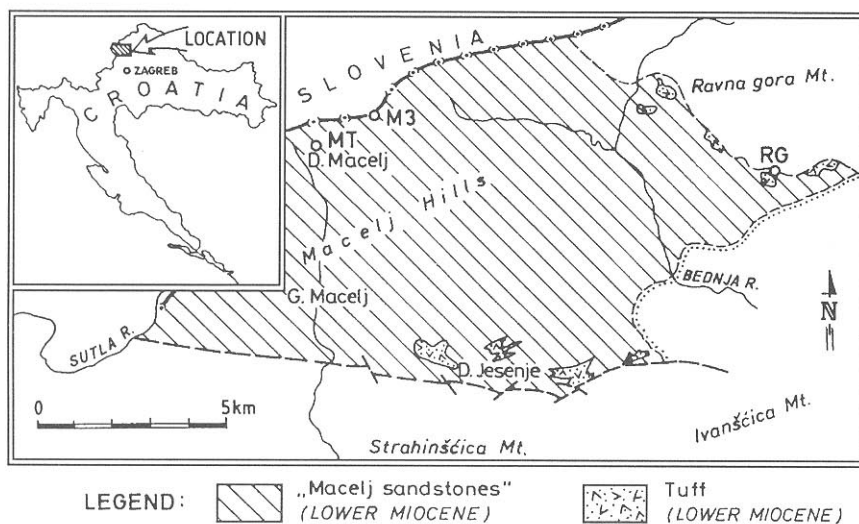


Fig. 1 Location map (modified from ŠIMUNIĆ et al., 1990).

Sample M3 is a glauconitic sandstone composed of poorly sorted, mostly angular, rarely subrounded fine-grained to medium-grained particles (0.3-0.7 mm in size). The detritus consists mostly of rock fragments with subordinate undulatory quartz, and very rare feldspars. The most common accessory mineral is garnet which is accompanied by subordinate tourmaline, apatite, muscovite, biotite and limonite aggregates. A greenish glauconitic matrix is predominant, together with dense chlorite-sericite aggregates, which are probably a diagenetic product of clays rich in organic impurities. Calcite cement occurs sporadically in intergranular pores. Rock fragments are mostly grains of quartzite, chert, crystalline schists, and occasionally macrocrystalline dolomite. The undulatory extinction of quartz grains indicates its metamorphic origin. Feldspars are almost completely sericitized; rare relict grains display zoning or dense polysynthetic twinning and corroded edges. Fragments of extrusive rocks, with plagioclase phenocrysts and micas produced by devitrification of volcanic glass were also identified. Some fissures in the detrital grains are slightly greenish.

Glauconitic material occurs in two basic forms: as detrital grains and as the matrix (Fig. 2a). Less commonly, the detrital glauconitic material occurs as well rounded grains composed of cryptocrystalline "grape like" darkgreen aggregates. Most of the glauconitic matrix material fills intergranular pores, is much brighter in colour and occurs as cryptocrystalline, platy-shaped aggregates, with single minute sericite and chlorite plates within the glauconitic material. The glauconitic matrix is not evenly distributed throughout the rock, but is rather concentrated in the shape of laminae and interlayers within the sandstone. Often there are layers composed nearly entirely of glauconitic matrix and interlayers in which the glauconitic material is almost absent. The glauconitic matrix displays features of plastic deformation and compact squeezing (e.g. sand grains which are nearly completely wrapped in glauconitic material).

Sample RG is very similar to sample M3, particularly in the composition of detrital grains, which are better sorted, subrounded to rounded, with size characteristics of medium-grained to coarse-grained sand.

The glauconitic material occupies intergranular pores in the parts that are clast or matrix supported. In contrast to samples M3 and MT, there is no glauconitic material in the form of detrital grains. The glauconitic material occurs in the matrix and it is most probably a product of glauconitization of fine volcanic ash or glass. The glauconitic material displays features of sedimentation under semiplastic conditions. Texturally, three types of the green glauconitic matrix can be distinguished: darkgreen grapy aggregates (Fig. 2b), yellowgreen, more or less homogeneous cryptocrystalline aggregates, with weak pleochroism and with sparse mica, and fibrous green aggregates with strong pleochroism which are probably produced by glauconitization of chlorite (Fig. 2b). In the RG sandstone, altered grains are present in which cryptocrystalline quartz dominates and which are slightly green along fissures (Fig. 2b).

Sample MT is a cross-laminated fine-grained to medium-grained sandstone, with mainly angular to subrounded grains, rarely with rounded grains, averaging 0.1-0.4 mm in size. The sandstone is composed of siliclastic grains, glauconitic material and matrix with sporadic calcite cement. In contrast to the previously described samples, siliclasts of MT sandstone consist of angular to subangular quartz fragments mainly with undulatory extinction. Clasts of quartzite, chert and low-metamorphic to medium-metamorphic grade schists (quartz-schists) are common, while to a lesser extent fragments of gneiss, mica-schist, dolomite, siltstone and sodic plagioclase are also present. In this sample, detrital flakes of muscovite are quite frequently observed.

Glauconitic material occurs mainly in the intergranular pores of siliclasts as cryptocrystalline matrix or as microcrystalline, platy yellow-olive-green aggregates

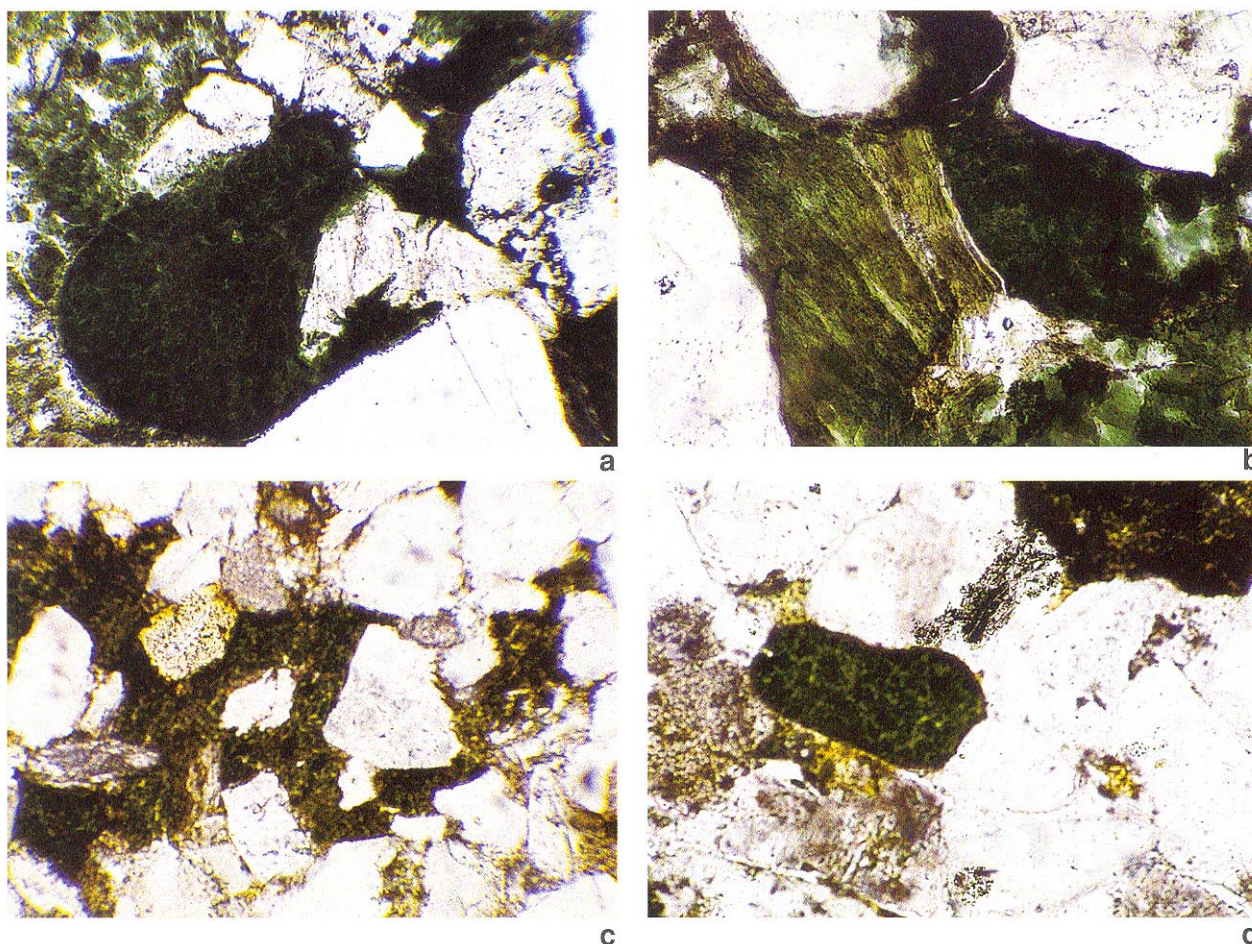


Fig. 2 a) Dark green grape-like detritic glauconitic material and light green glauconitic matrix filling intergranular pores. Thin section of sample M3; 1N, photo length 1.36 mm. b) Glauconitic matrix in the form of dark-green grape-like clusters and green fibrous clusters. Light green glauconitic material coatings in quartz fractures are also present. Thin section of sample RG; 1N, photo length 0.86 mm. c) Laminae with glauconitic matrix. Thin section of sample MT; 1N, photo length 1.36 mm. d) Detritic grape-like dark-green glauconitic grain. Thin section of sample MT; 1N, photo length 0.86 mm.

(Fig. 2c). The structure and relationship of the glauconitic material with these siliciclasts indicates that the groundmass was originally composed of fine volcanic ash or semilithified glassy tuff. The glauconitic mass frequently contains fine-dispersed pyrite and organic matter. The glauconitic material matrix is commonly concentrated within single laminae. Glauconitic material rarely occurs in the form of spherical and grape-like grains (Fig. 2d), which can be distinguished from the glauconitic matrix due to their more intense green colour, and the lack of any internal microtexture except cryptocrystalline and microcrystalline aggregates.

Despite some small differences, all the examined sandstones (M3, RG and MT) according to PETTIJOHN et al. (1972) can be classified as lithic graywackes.

XRD analysis, carried out on bulk-rock samples, shows that quartz is the dominant mineral in sample M3, which also contains a considerable amount of calcite, subordinate plagioclase and K-feldspar, two chemically different types of dolomite, and minor quantities of muscovite and siderite. The amount of glauconitic material is very small. The mineral composition of sample RG differs from the M3 sample since it contains

several times the amount of glauconitic material and considerably less calcite. Sample RG also contains two different dolomite types, some more plagioclase, a little chlorite, muscovite, and no siderite. The highest content of quartz and muscovite are present in sample MT which also contains dolomite and some calcite, plagioclase, K-feldspar, chlorite and haematite. The content of glauconitic material is higher in sample MT than in sample M3.

3. SEPARATION OF PURE GLAUCONITIC MATERIAL AND EXPERIMENTAL METHODS

XRD patterns of the analysed bulk-rock sandstones samples could not be used to identify the glauconitic material due to the relatively small amounts present in the samples. Separation of pure glauconitic material was carried out, to enable further determination to be undertaken.

After fragmentation, sieving and water washing, the 0.1-0.2 mm and 0.2-0.315 mm fractions were enriched in glauconitic material. These were later magnetically separated by a Frantz isodynamic separator. The mag-

netic glauconitic fractions were obtained at $I = 0.40\text{--}0.55$ A (labelled MT/1, M3/1 and RG/1) and at $I = 0.55\text{--}0.60$ A (labelled M3/2 and RG/2), and were finally purified by hand-picking under the binocular microscope. Other magnetic fractions of analysed samples contained more impurities consisting of other sandstone mineral constituents mixed with glauconitic material. After a purity check using XRD, small quantities of carbonate (dolomite, siderite, calcite) and amorphous Fe-compositions were removed from the M3/2, RG/2, M3/1 and MT fractions with diluted hydrochloric acid. A method to obtain pure glauconitic material from pulverised glauconitic material fractions (after separation in a Frantz isodynamic separator) using sedimentation from a water suspension was tested. The fraction $<1\ \mu\text{m}$ was separated. The purity of glauconitic material from sample M3/2 obtained by this method was much higher than that obtained by hand-picking. The glauconitic material obtained in this way was used in further analysis. Other samples purified using the same method gave fractions of equal or less purity than the fractions obtained by hand-picking.

Fractions M3/1 and M3/2 are equally distributed in separated glauconitic material of M3 sample. In the M3/1 fraction the grains are mainly subrounded to rounded in shape. In the RG sample about 4/5 of the total glauconitic material content is in the fraction RG/1 and about 1/5 in the fraction RG/2. In the MT sample almost all of separated glauconitic material is in the

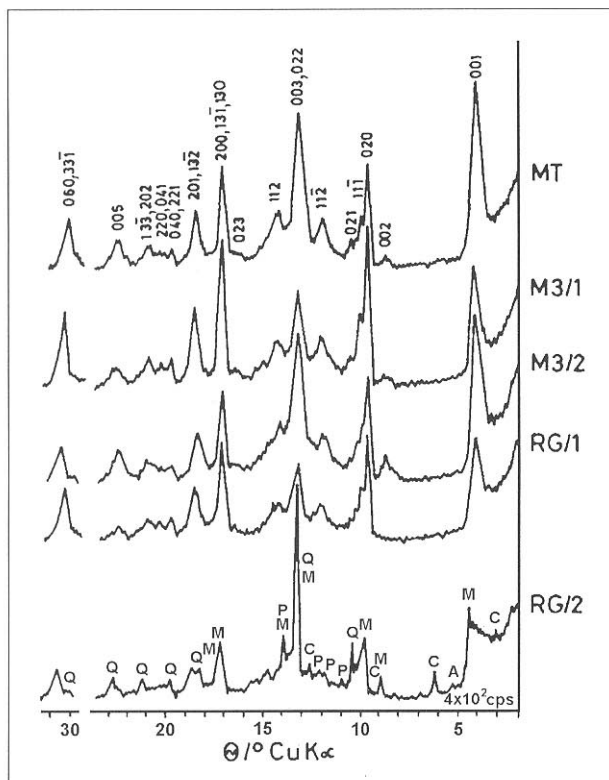


Fig. 3 XRD powder patterns of separated glauconite samples. The indices of diffraction lines of glauconitic material are indicated in the pattern of sample MT. C = chlorite; M = muscovite; A = amphibole; Q = quartz; P = plagioclase.

MT/1, so only this fraction was analysed as representing sample MT.

Depending on the increasing of magnetism the colour of the glauconitic material fraction ranges from light to very dark green. The M3 and MT glauconitic materials have a prominent blue shade whereas the RG fractions have a grass green colour, particularly when pulverised.

Separated pure or nearly pure glauconitic material fractions (samples MT, M3/1, M3/2, RG/1 and RG/2) were analysed chemically, thermally and by XRD.

XRD powder investigations were done on a Philips diffractometer, using $\text{CuK}\alpha$ radiation, a graphite monochromator and proportional counter. Diffraction patterns of randomly oriented air dried samples, and specimens with preferred orientation (air dried samples and samples treated by ethylene glycol) were recorded.

Comparing glauconite/smectite and illite/smectite interlayered minerals VELDE & ODIN (1975) concluded that "illite and glauconite mixed layered phases appear to be crystallographically similar." Therefore we used the method for identification of illitic material by ŠRODOŃ (1984) and ŠRODOŃ & EBERL (1984) to identify the glauconitic material in this study. ŠRODOŃ (1984) used this method for the identification of one glauconite sample (sample No 39 in table 2 of cited paper), too. According to them the ratio for pure illite is determined as follows:

$$I_r = \frac{I(001)/I(003) \text{ (air dried sample)}}{I(001)/I(003) \text{ (glycolated sample)}} = 1.$$

If the illitic material is expandable I_r will increase, i.e. the ratio increases with increasing amounts of the expandable component. With regard to layer interstratification, the glauconite-smectite series is similar to the illite-smectite series. For this reason the I_r ratio has been used in this paper for comparison of glauconitic materials.

The chemical analysis of separated glauconitic material was performed by classical chemical methods, while sodium and potassium were determined using a flame photometer. Cation exchange capacity (CEC) was determined according to Kjeldahl (cit. ŠUŠTERČIĆ, 1969) with previous replacement of exchangeable cations using ammonium acetate.

Thermal analyses (DTA, TG, DTG) were performed by the MOM derivatograph, Budapest, with a heating rate of cca $10^\circ\text{C}/\text{min}$. To decrease the influence of relative moisture contents, samples were stored in the desiccator for 24 hours before analysis. The weight of each sample used in the individual thermal analysis was 0.23 g. The weight loss due to dehydration was read from TG curves according to SCHULTZ (1969).

4. RESULTS

XRD powder patterns of randomly oriented and oriented separated glauconitic material are shown in Figs.

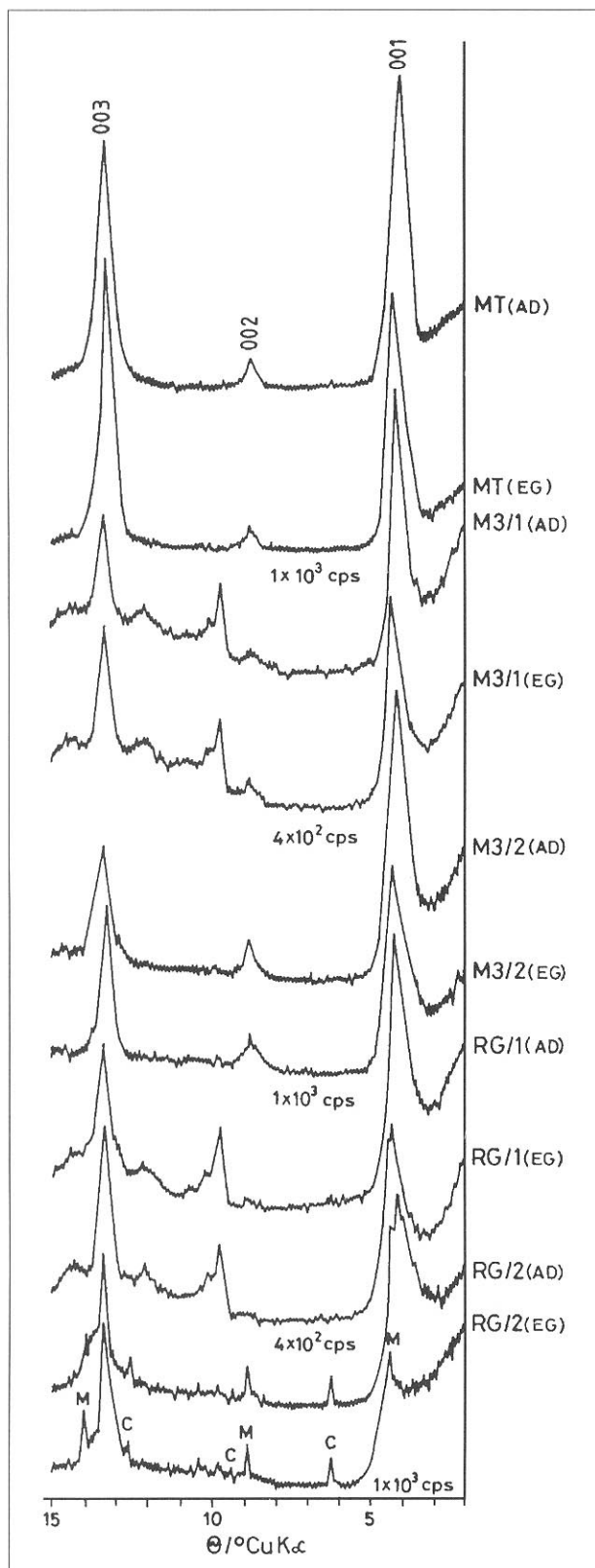


Fig. 4 XRD powder patterns of oriented samples. AD - air dried sample; EG - ethylene glycol treated sample; M = muscovite; C = chlorite.

3 and 4, which illustrate that samples MT, M3/1, M3/2 and RG/1 contain practically no impurities. In contrast, sample RG/2 contains numerous impurities (chlorite, muscovite, amphibole, quartz, and plagioclase). The same impurities are present in the $< 1 \mu\text{m}$ fraction of

the RG/2 sample, indicating a close relationship of glauconitic material and initial substrate of glauconitization. Diffraction patterns also show that this sample contains the highest quantity of expanding layers.

Results of chemical analysis and crystallochemical formula calculated on the basis of $\text{O}_{10}(\text{OH})_2$ are presented in Table 1.

The Ir-values are presented in Table 2.

Thermoanalytical curves of separated glauconitic materials are shown in Fig. 5. The DTA curves display three endothermic effects; the first in the temperature interval from 100°C to 200°C which corresponds to dehydration; the second in temperature interval from 450°C to 600°C which corresponds to dehydroxylation, and the third, a weak effect at $\sim 900^\circ\text{C}$ which indicates disintegration of structure. According to UTSAL & UTSAL (1981) a weak exothermic effect at $360\text{--}380^\circ\text{C}$ may be indicative of the oxidization of structural Fe^{2+} . However, this effect is more obviously expressed in weakly magnetic fractions, although their FeO contents do not differ essentially in weakly and strongly magnetic fractions of the relevant samples. For this reason it is more probable that the exothermic effects mentioned above, indicate the presence of impurities that are not detected by XRD.

Dehydration and dehydroxylation endothermic effects are accompanied by an equivalent weight loss on TG curves. Besides the TG curves the total weight losses are also marked in Fig. 5. The weight losses related to adsorbed and structural water, which were determined according to SCHULTZ (1969), are presented in Table 2.

5. DISCUSSION

The AIPEA Nomenclature Committee (BAILEY et al., 1979; BAILEY, 1980) have defined glauconite as an Fe-rich dioctahedral mica with tetrahedral Al (or Fe^{3+}) greater than 0.2 atoms per formula unit and octahedral R^{3+} correspondingly greater than 1.2 atoms. The interplanar spacing $d(060)$ is $> 1.510 \text{ \AA}$. Additional characteristics of glauconite are that the octahedral charge is greater than +5.3 per formula unit and that the interlayer charge in non-expandable specimens varies from $\approx +0.8$ to $+0.9$ (BAILEY et al., 1984). According to the AIPEA Nomenclature Committee the species glauconite is a single-phase and, ideally, is not interstratified. Specimens with expandable layers can be described as randomly interstratified glauconite-smectite. BUCKLEY et al. (1978) proposed that the term "glauconite" should be used only for those minerals containing less than 5% interlayering. According to the same authors glauconites have mainly the $1Md$ type of structure as indicated by extended basal and reduced hkl reflections on their XRD powder patterns. Structural imperfections of glauconites have previously been attributed to interstratification. The heterogeneity in the composition and structure of glauconite pellets was

	MT	M3/1	M3/2	RG/1	RG/2
SiO ₂	51.74	52.14	51.57	50.58	52.94
TiO ₂	0.10	0.15	0.21	0.16	0.26
Al ₂ O ₃	6.14	11.42	16.44	9.33	10.94
Fe ₂ O ₃	18.98	13.03	8.60	18.46	15.84
FeO	4.24	2.17	2.68	2.57	1.97
MgO	3.23	5.17	2.07	3.45	2.21
CaO	0.38	0.62	0.59	0.80	1.39
Na ₂ O	0.29	0.35	0.55	0.41	0.40
K ₂ O	8.35	7.81	6.27	7.28	4.88
H ₂ O ¹⁰⁵	1.51	2.24	5.01	2.90	5.21
LOI	5.20	4.85	6.24	4.63	4.45
Total	100.16	99.96	100.23	100.57	100.49
Si	3.79	3.70	3.71	3.66	3.80
Al	0.21	0.30	0.29	0.34	0.20
Al	0.32	0.66	1.11	0.46	0.72
Fe ³⁺	1.05	0.70	0.47	1.01	0.85
Fe ²⁺	0.26	0.13	0.16	0.16	0.12
Mg	0.35	0.55	0.22	0.37	0.24
Ti	0.01	0.01	0.01	0.01	0.01
Ca	0.03	0.05	0.05	0.06	0.11
Na	0.04	0.05	0.08	0.06	0.06
K	0.78	0.71	0.58	0.67	0.45
Σ (R ²⁺ R ³⁺)	1.99	2.05	1.97	2.01	1.94
Σ R ³⁺	1.37	1.36	1.58	1.47	1.57
Σ A	0.85	0.81	0.71	0.79	0.62

Table 1 Chemical analyses and the number of ions per O₁₀(OH)₂.

used to explain the existence of a series from 1M to 1Md type structure (BURST, 1958; HOWER, 1961; BENTOR & KASTNER, 1965). However, SAKHAROV et al. (1990) demonstrated that homogenous glauconites without expandable layers can also give weak and broad *hkl* reflections due to the presence of structural defects resulting from various types of 2:1 layer stacking faults. For this reason, the amount of expanding layers must be also determined in glauconite samples. Numerous authors determined that as the K and Fe³⁺ contents decrease, the amount of Al^{VI} increases together with the number of expandable layers (ODOM, 1984).

In the present study the proportions of expandable layers (Table 2) have been estimated using the CEC values (MANGHANI & HOWER, 1964) and the K content (THOMPSON & HOWER, 1975) and by comparison of XRD patterns of glycol-solvated samples with computer calculated diffraction profiles given by THOMPSON & HOWER (1975). The estimated proportions of expandable layers are also fairly compatible with the contents of adsorbed water and the Ir-values (Table 2).

For all samples studied in this paper Ir > 1 (Table 2). According to the method of ŠRODONÍ (1984) and ŠRODONÍ & EBERL (1984) the plotted 002 and 003

Sample	Percentage of expandable layers			CEC mEq/100g	K ions per O ₁₀ (OH) ₂	Ir	Weight losses / % according TG curves	
	from CEC ¹	from K content ²	from XRD ²				adsorbed water	structural water
MT	0	5	5	7.1	0.78	1.40	1.42	4.68
M3/1	5	> 5	5	10.2	0.71	1.61	2.16	4.62
M3/2	12	10-15	10	15.6	0.58	1.93	3.79	4.62
RG/1	< 10	< 10	< 10	12.1	0.67	1.87	2.82	4.34
RG/2	35-40	nd	40	31.5	0.45	nd	5.09	4.23

Table 2 The contents of expandable layers and corresponding parameters for their estimation. Legend: ¹ according MANGHANI & HOWER (1964); ² according THOMPSON & HOWER (1975); nd - not determined.

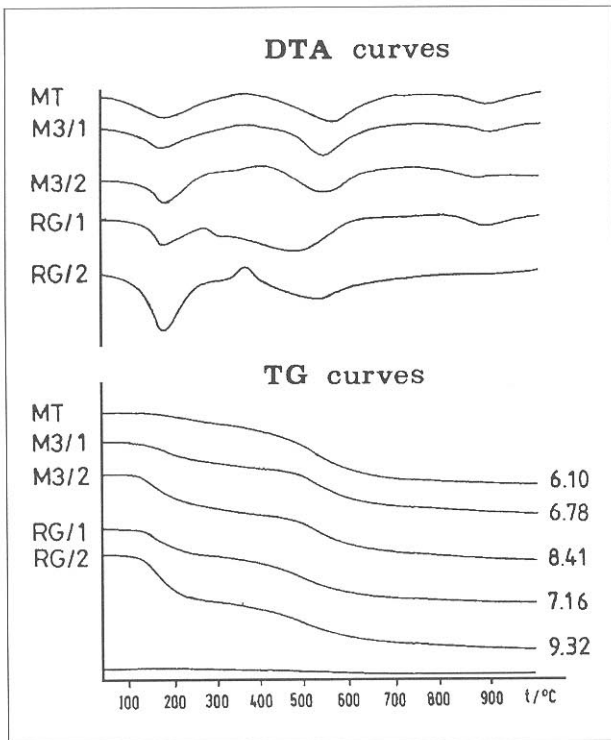


Fig. 5 Thermoanalytical curves of glauconite samples. Weight loss curves include corrections from blank curve (at the bottom of figure). Percent weight losses are indicated along TG curves.

reflex positions of glycolated samples fell in the illite field or very close to it (Fig. 2 in ŠRODOŇ, 1984). No samples plotted in the illite/smectite (I/S) field. Therefore, according to ŠRODOŇ (1984) and ŠRODOŇ & EBERL (1984) all analysed samples (except RG/2) present the same type of illitic (in our paper glauconitic) material: mixtures of pure illite (respectively glauconite) and an ISII-ordered mineral with < 15% S.

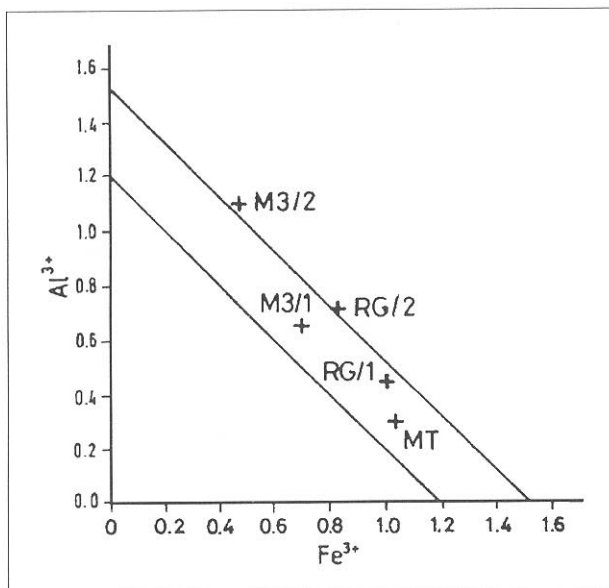


Fig. 6 Trivalent octahedral ion contents (R^{3+}) per formula unit. Solid lines indicate limits of glauconite R^{3+} content (modified from BUCKLEY et al., 1984).

In relation to K content, the MT sample is practically non-interstratified. Sample M3/2 contains more smectite layers according to the K content and CEC value (Table 2). It has higher expandability than suggested by the results of ŠRODOŇ (1984) and ŠRODOŇ & EBERL (1984) method.

Sample MT contains only a few expandable layers (Table 2) and its structural chemical formula is very close to the average formula of unaltered glauconites analysed by BUCKLEY et al. (1978). This is confirmed also by its plot on the Al^{VI} - Fe^{3+} diagram (Fig. 6), as well as its position on the diagram which displays the relation of $d(060)$ spacings to Fe^{3+} ions (Fig. 7). The XRD pattern (Fig. 3) indicates a $1Md$ type structure; however, among all samples analysed in the present study, the MT sample has the less reduced hkl reflections. All these parameters indicate that the MT sample in fact almost represents single-phase glauconite.

Samples M3/1 and M3/2 have $1Md$ structure (Fig. 3). Sample M3/1 contains a little bit more than 5%, and sample M3/2 contains 10% to 15% smectitic layers (Table 2). According to THOMPSON & HOWER (1975) both samples show "IMII" type of ordering. The relationship between the number of octahedral Al^{3+} and Fe^{3+} ions for both samples corresponds to glauconite. Sample M3/2 plots very near to the boundary of the glauconite field (Fig. 6). The high Al^{VI} content of both samples gives rise to the small $d(060)$ values: 1.511 Å (M3/1) and 1.510 Å (M3/2). These values are very close to the celadonite-glauconite boundary as proposed by BUCKLEY et al. (1978), but on the Fe^{3+} vs. $d(060)$ diagram, both samples plot within the glauconite field (Fig. 7).

Due to the small amount of expandable layers in sample M3/1, the average chemical composition of non-expandable layers in it is not essentially different from the bulk chemical composition presented in Table 1. It was not possible to determine the average chemical composition of non-expandable layers in sample M3/2, but due to very high Al^{VI} content in the bulk sample (Table 1), it probably corresponds to Al-glauconite.

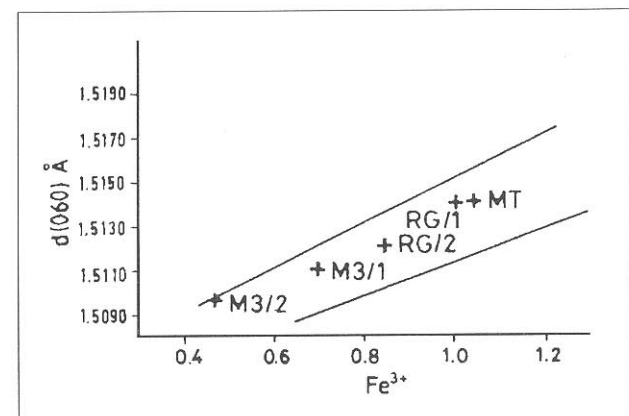


Fig. 7 Relationship of $d(060)$ spacing to Fe^{3+} ions. Solid lines indicate approximate limits of glauconite (modified from BUCKLEY et al., 1984).

Samples M3/1 and M3/2 per formula unit contain 0.66 and 1.11 Al^{VI} atoms and 0.55 and 0.22 Mg atoms, respectively (Table 1). The large differences in the octahedral atom content between the two fractions of sample M3 cannot be explained either by differences in the amount of expanding layers ($\Delta \approx 10\%$), or by differences in the degree of maturity of glauconite. This difference in chemical composition indicates either different initial substrates of glauconitization, or different environments of glauconitization. Microscopic data and differences in the shape and colour of separated grains suggest that detrital glauconitic material is predominant in the M3/1 fraction whereas the matrix glauconitic material is predominant in fraction M3/2.

RG samples have essentially different XRD patterns (Figs. 3 and 4). The RG/1 sample has *1Md* type of structure and contains < 10% expandable layers, and according to THOMPSON & HOWER (1975) shows an "IMII" type of ordering. In the octahedral Al³⁺-Fe³⁺ ion diagram (Fig. 6) and in the *d*(060)-Fe³⁺ diagram (Fig. 7), the sample plots in the glauconite field very close to sample MT.

The glauconite component in the RG/2 sample contains 35-40% expandable layers and, according to THOMPSON & HOWER (1975), represents randomly interstratified glauconite-smectite. Chemical comparison between samples RG/1 and RG/2 is not possible because sample RG/2 contains impurities and therefore, the chemical composition of smectite is unknown. However, on the basis of optical analysis it is presumed that glauconitic material from sample RG/1 (predominantly in the form of dark-green grapy aggregates) and RG/2 (probably other types of glauconitic matrix) represent different phases of an evolved glauconite series originated from same or similar initial substrate of glauconitization. Microscopic observations (Fig. 2b) and the mineral composition determined by XRD (Fig. 3) suggest that the glauconitic material from the RG/2 is a product, at least partly, of chlorite and probably muscovite glauconitization.

In concordance with ODIN & MATTER (1981) and ODIN & FULLAGAR (1988) we identify these stages of glauconitization for analysed "glauconitic minerals": evolved to highly evolved (MT and M3/1), evolved (RG/1), slightly evolved to evolved (M3/2) and slightly evolved (RG/2).

6. CONCLUSIONS

The Macelj-sandstones were deposited in shallow-marine environments on foreshores, shorefaces, and tidal flats with or without deltas at stream and small river mouths. The detritus load for the marine shoals,

which were often separated from the open sea by sandy bars and tidal flats, is debris transported by rivers from areas of active erosion. Periodic but explosive synsedimentary dacite-andesite volcanism made possible tuff accumulation (for example, in the area of Donje Jeseenje) and the presence of great quantities of volcanoclastic material within the epiclastic detritus. The volcanoclastic material in the detritus was deposited either directly during volcanic eruptions, or by its re-deposition and accumulation with the detritus of the Macelj-sandstones.

Data obtained from analysis of 3 samples of the Macelj-sandstones show that there are differences not only among glauconitic material from various locations but also among glauconitic material from the same sandstone sample. These differences are already noticeable from the microscopic examination of sandstones and after glauconite separation. In the strongly magnetic fractions the glauconitic material has a darker green colour than the weakly magnetic fraction and, based on analytical data, the former is more evolved. In the series from highly evolved to less evolved glauconitic materials, the proportions of expanding layers increase from < 5% to approximately 40%.

Heterogeneity of the M3 sandstone relates to the magnetic features of glauconitic material and the presence of detrital glauconitic grains point to redeposition during glauconitization. Significant differences between the chemical composition of samples M3/1 and M3/2, particularly in Al, Fe and Mg proportions, may suggest differences in the initial substrate of glauconitization from sample M3 as well as differences in comparison with glauconitic material from samples RG and MT. The detected mineralogical differences between glauconitic material from sample M3 are consistent with the microscopic data which indicates redeposition of an unconsolidated sediment. Chemical differences of magnetically more homogeneous glauconitic material from sandstone RG may be explained by differences in chemical and structural features within the evolving series of glauconites which originated in the same glauconitization cycle, from probably the same or similar initial substrate. In the MT sample only one single magnetic fraction was obtained and thus it can be presumed that the substrate of glauconitization was uniform in composition.

The results obtained from this investigation neither deny nor confirm the results achieved by other investigators (TIŠLJAR & ŠIMUNIĆ, 1978; ŠIMUNIĆ et al., 1990), indicating that glauconitic material from the examined Macelj-sandstones were probably produced by alteration of dacite-andesite volcano-clastic material in shallow-marine environments.

7. REFERENCES

- BAILEY, S.W. (1980): Summary of recommendations of AIPEA Nomenclature Committee.- *Clay Miner.*, 15, 85.
- BAILEY, S.W., BRINDLEY, G.W., FANNING, D.S., KODAMA, H. & MARTIN, R.T. (1984): Report of the Clay Minerals Society Nomenclature Committee for 1982 and 1983.- *Clays Clay Miner.*, 32, 239.
- BAILEY, S.W., BRINDLEY, G.W., KODAMA, H. & MARTIN, R.T. (1979): Report of the Clay Minerals Society Nomenclature Committee for 1977 and 1978.- *Clays Clay Miner.*, 27, 238-239.
- BENTON, Y.K. & KASTNER, M. (1965): Notes on the mineralogy and origin of glauconite.- *J. Sed. Petrol.*, 35, 155-166.
- BUCKLEY, H.A., BEVAN, J.C., BROWN, K.M., JOHNSON, L.R. & FARMER, V.C. (1978): Glauconite and celadonite: two separate mineral species.- *Mineral. Mag.*, 42, 373-382.
- BUCKLEY, H.A., EASTON, A.J. & JOHNSON, L.R. (1984): Compositional variations in glauconite.- *Mineral. Mag.*, 48, 119-126.
- BURST, J.F. (1958): Mineral heterogeneity in "glauconite" pellets.- *Amer. Mineral.*, 43, 481-497.
- GORJANOVIĆ-KRAMBERGER, D. (1904): Geologijska prijedlogna karta Kraljevine Hrvatske i Slavonije. Rogatec-Kozje (Zona 21, Col. XIII) 1:75.000 (Geologische Übersichts-Karte des Königreiches Kroatien-Slavonien. Rohitsch-Drachenburg).- *Izd. Kr. hrv. slav. dalmat. zemaljska vlada, Odio za unutarnje poslove, Zagreb.*
- HOWER, J. (1961): Some factors concerning the nature and origin of glauconite.- *Amer. Mineral.*, 46, 313-334.
- MANGHANI, M. & HOWER, J. (1964): Glauconites: cation exchange capacities and infrared spectra.- *Amer. Mineral.*, 49, 586-598.
- ODIN, G.S. & FULLAGAR, P.D. (1988): Geological significance of the glaucony facies.- In: ODIN, G.S. (ed.): *Green marine clays. Developments in Sedimentology*, 45, 295-332, Elsevier, Amsterdam-Oxford-New York-Tokyo.
- ODIN, G.S. & MATTER, A. (1981): De glauconiarum origine.- *Sedimentology*, 28, 611-641.
- ODOM, E. (1984): Glauconite and celadonite minerals.- In: *Micas. Reviews in Mineralogy*, 13, 545-572, Mineral. Soc. America.
- PETTIJOHN, F.J., POTTER, P.E. & SIEVER, R. (1972): *Sand and sandstones.*- Springer-Verlag, New York-Heidelberg-Berlin, 615 p.
- SAKHAROV, B.A., BESSON, G., DRITS, V.A., KAMENEVA, M.Yu., SALYN, A.L. & SMOLIAR, B.B. (1990): X-ray study of the nature of stacking faults in the structure of glauconites.- *Clay Miner.*, 25, 419-435.
- SCHULTZ, L.G. (1969): Lithium and potassium absorption, dehydroxylation temperature, and structural water content of aluminous smectites.- *Clays Clay Miner.*, 17, 115-149.
- ŠRODOŃ, J. (1984): X-ray powder diffraction identification of illitic materials.- *Clays Clay Miner.*, 32, 337-349.
- ŠRODOŃ, J. & EBERL, D.D. (1984): Illite.- In: *Micas. Reviews in Mineralogy*, 13, Mineral. Soc. America.
- ŠIMUNIĆ, AI., AVANIĆ, R. & ŠIMUNIĆ, An. (1990): "Maceljski pješčenjaci" i vulkanizam zapadnog dijela Hrvatskog Zagorja (Hrvatska).- *Rad JAZU*, 449, (Raz. za prirod. znan., 24), 179-194.
- ŠUŠTERČIĆ, N. (1969): *Pogonske analize.*- Školska knjiga, Zagreb, 221 p.
- THOMPSON, G.R. & HOWER, J. (1975): The mineralogy of glauconite.- *Clays Clay Miner.*, 23, 289-300.
- TIŠLJAR, J. & ŠIMUNIĆ, AI. (1978): *Maceljski pješčenjaci.*- Vodič ekskurzije III Skupa sedimentologa Jugoslavije, Hrvatsko geol. društvo, Zagreb, 32-37.
- UTSAL, K. & UTSAL, V. (1981): Isledovanie izmene-nia okraski, formi i strukturnih osobenostej glaukonita Estonii pri raznih temperaturah do 1500°C.- *Tartu Ülikooli toimetised, Uč. zap. Tartus UN-TA*, 561, 50-71.
- VELDE, B. & ODIN, G.S. (1975): Further informations related to the origin of glauconite.- *Clays Clay Miner.*, 23, 376-381.

Manuscript received May 19, 1995.

Revised manuscript accepted April 28, 1997.

